

# Selective 14-3-3 $\gamma$ induction quenches p- $\beta$ -catenin Ser37/Bax-enhanced cell death in cerebral cortical neurons during ischemia

XJ Lai<sup>1</sup>, SQ Ye<sup>1</sup>, L Zheng<sup>1</sup>, L Li<sup>1</sup>, QR Liu<sup>1</sup>, SB Yu<sup>1</sup>, Y Pang<sup>2</sup>, S Jin<sup>3</sup>, Q Li<sup>4</sup>, ACH Yu<sup>2</sup> and XQ Chen<sup>\*1</sup>

Ischemia-induced cell death is a major cause of disability or death after stroke. Identifying the key intrinsic protective mechanisms induced by ischemia is critical for the development of effective stroke treatment. Here, we reported that 14-3-3 $\gamma$  was a selective ischemia-inducible survival factor in cerebral cortical neurons reducing cell death by downregulating Bax dependent direct 14-3-3 $\gamma$ /p- $\beta$ -catenin Ser37 interactions in the nucleus. 14-3-3 $\gamma$ , but not other 14-3-3 isoforms, was upregulated in primary cerebral cortical neurons upon oxygen–glucose deprivation (OGD) as measured by quantitative PCR, western blot and fluorescent immunostaining. The selective induction of 14-3-3 $\gamma$  in cortical neurons by OGD was verified by the *in vivo* ischemic stroke model. Knocking down 14-3-3 $\gamma$  alone or inhibiting 14-3-3/client interactions was sufficient to induce cell death in normal cultured neurons and exacerbate OGD-induced neuronal death. Ectopic overexpression of 14-3-3 $\gamma$  significantly reduced OGD-induced cell death in cultured neurons. Co-immunoprecipitation and fluorescence resonance energy transfer demonstrated that endogenous 14-3-3 $\gamma$  bound directly to more p- $\beta$ -catenin Ser37 but not p-Bad, p-Ask-1, p-p53 and Bax. During OGD, p- $\beta$ -catenin Ser37 but not p- $\beta$ -catenin Ser45 was increased prominently, which correlated with Bax elevation in cortical neurons. OGD promoted the entry of 14-3-3 $\gamma$  into the nuclei, in correlation with the increase of nuclear p- $\beta$ -catenin Ser37 in neurons. Overexpression of 14-3-3 $\gamma$  significantly reduced Bax expression, whereas knockdown of 14-3-3 $\gamma$  increased Bax in cortical neurons. Abolishing  $\beta$ -catenin phosphorylation at Ser37 (S37A) significantly reduced Bax and cell death in neurons upon OGD. Finally, 14-3-3 $\gamma$  overexpression completely suppressed  $\beta$ -catenin-enhanced Bax and cell death in neurons upon OGD. Based on these data, we propose that the 14-3-3 $\gamma$ /p- $\beta$ -catenin Ser37/Bax axis determines cell survival or death of neurons during ischemia, providing novel therapeutic targets for ischemic stroke as well as other related neurological diseases.

*Cell Death and Disease* (2014) 5, e1184; doi:10.1038/cddis.2014.152; published online 17 April 2014

**Subject Category:** Neuroscience

Ischemia-induced cell death is a major cause of disability and death in the elderly worldwide.<sup>1,2</sup> After ischemic stroke, major cell death occurs during 6 h of early ischemic stage,<sup>3</sup> although sparse delayed cell death 24 h after ischemia lasts for a longer time.<sup>2</sup> Thrombolytic therapy is the only clinically effective treatment for stroke; however, it must be performed within 4 h after the onset of stroke before massive cell death appears.<sup>1,4–6</sup> Therefore, reducing cell death or injury during early ischemic stage to elongate the therapeutic time window for thrombolysis is of primary importance in treating stroke.<sup>7</sup> Unfortunately, there is not such clinically effective cytoprotective drug discovered until now. Tested cytoprotective drugs aiming to reduce free radical and calcium overloads that occur mainly during ischemic reperfusion are clinically ineffective,<sup>8,9</sup>

reflecting a major inadequacy in targeted damaging factors as differential cell death mechanisms are involved in different kinds of brain cells during ischemia or reperfusion. For example, it is well known that astrocytes and neurons respond differently to ischemic insults via distinct mechanisms.<sup>10</sup> Theoretically, protecting all types of brain cells simultaneously is required for stroke treatment.<sup>2</sup> Thus, finding the key protective molecules conserved in brain cells and understanding clearly their protective mechanisms is required for future development of effective cytoprotective drugs and treatments.

14-3-3 families are highly conserved scaffold proteins and are essential for cell survival, as deletion of all 14-3-3 isoforms is lethal in yeast and mice.<sup>11,12</sup> Knockdown of 14-3-3 $\zeta$  alone is sufficient to induce cell death in lung cancer cells,<sup>13</sup>

<sup>1</sup>Department of Pathophysiology, School of Basic Medicine, Key Laboratory of Neurological Diseases, Ministry of Education, Hubei Provincial Key Laboratory of Neurological Diseases, Huazhong University of Science and Technology, Wuhan, China; <sup>2</sup>Neuroscience Research Institute, Department of Neurobiology, School of Basic Medical Sciences, The Key Laboratory of Neuroscience, The Ministry of Education and Ministry of Health (PKU), Peking University, Beijing, China; <sup>3</sup>Department of Pharmacology, School of Basic Medicine, Huazhong University of Science and Technology, Wuhan, China and <sup>4</sup>Translational Medical Center for Development and Disease, Institute of Pediatrics, Children's Hospital of Fudan University, Shanghai, China

\*Corresponding author: XQ Chen, Department of Pathophysiology, School of Basic Medicine, Key Laboratory of Neurological Diseases, Ministry of Education, Hubei Provincial Key Laboratory of Neurological Diseases, Huazhong University of Science and Technology, 13 Hangkong Road, Wuhan 430030, China. Tel/Fax: +86 27 83692608; E-mail: chenxiaojian66@gmail.com

**Keywords:** 14-3-3;  $\beta$ -catenin; Bax; neuron; astrocyte; stroke

**Abbreviations:** OGD, oxygen and glucose deprivation; pMCAo, permanent middle cerebral artery occlusion; Ipsi, ipsilateral cortex; Contra, contralateral cortex; qPCR, quantitative polymerase chain reaction; Difopein, dimeric 14-3-3 peptide inhibitor; YFP, yellow fluorescent protein; MCL-1, myeloid cell leukemia sequence-1; PI, propidium iodide; FRET, fluorescence resonance energy transfer; TTC, 2,3,5-triphenyltetrazolium chloride; shRNA, short hairpin RNA; Ask-1, apoptosis signal-regulating kinase 1

Received 02.11.13; revised 20.2.14; accepted 07.3.14; Edited by A Verkhratsky

suggesting that distinct 14-3-3 isoforms could determine cell fate. It is well known that 14-3-3 elicits antiapoptotic effects by interacting with various pro-apoptotic proteins such as Bad, Bax, p53 and Ask-1 in the cytoplasm depending on specific apoptotic cues.<sup>14–16</sup> In mammalian brains, six ( $\beta$ ,  $\epsilon$ ,  $\eta$ ,  $\gamma$ ,  $\tau$ ,  $\zeta$ ) of the seven 14-3-3 isoforms are highly expressed. In neurological diseases, such as Creutzfeldt–Jakob disease, the elevation of distinct 14-3-3 isoforms in the cerebral–spinal fluid is considered as a biological marker of the disease or predictor of its progression.<sup>17</sup> Malfunction of 14-3-3 is heavily associated with neurodegenerative diseases such as Alzheimer’s disease<sup>18</sup> and Parkinson’s disease<sup>19</sup> although the exact biological functions of 14-3-3 isoforms remain to be defined. We have previously reported that 14-3-3 $\gamma$  is selectively upregulated by oxygen–glucose deprivation (OGD) in cultured astrocytes and protects them from OGD-induced cell death via binding to p-Bad Ser112 selectively.<sup>20,21</sup> It is interesting to know whether 14-3-3 $\gamma$  could protect ischemic neurons via a similar mechanism or not as 14-3-3 $\gamma$  is expressed predominantly in neurons.

The present study aims to investigate the ischemic response and functional role of 14-3-3 isoforms in cerebral cortical neurons and to understand its underlying mechanisms. We demonstrated that OGD or ischemia selectively induced 14-3-3 $\gamma$  in cortical neurons, which was important in protecting neurons from ischemic cell death. Notably, 14-3-3 $\gamma$

bound specifically to more p- $\beta$ -catenin Ser37 in the nuclei to suppress Bax expression in neurons, differing from the previously reported antiapoptotic mechanisms of 14-3-3 $\gamma$  in astrocytes. Clearly, these differential protective mechanisms are important for the derivation of better preventions and treatments for stroke.

## Results

### Ischemia selectively upregulates the $\gamma$ -isoform of 14-3-3 in cortical neurons.

For analyzing the ischemic responses of 14-3-3 proteins in neurons, isoform-specific 14-3-3 antibodies were used. Results of western blot demonstrated that 14-3-3 $\beta$ ,  $\epsilon$ ,  $\eta$ ,  $\gamma$  and  $\zeta$  antibodies recognized the corresponding overexpressed 14-3-3 isoform only (Supplementary Figure 1). Then, we measured the expression of 14-3-3 isoforms in primary cultures of rat cerebral cortical neurons subjected to OGD. Results of western blot and statistical analysis demonstrated that  $\gamma$  but not  $\beta$ ,  $\epsilon$ ,  $\eta$  and  $\zeta$  isoforms of 14-3-3 was significantly increased upon 1, 2, 3 and 4 h of OGD incubation (Figure 1a). The results of fluorescent immunostaining also revealed an elevation of 14-3-3 $\gamma$  but not 14-3-3 $\beta$ ,  $\epsilon$ ,  $\eta$  and  $\zeta$  in primary cortical neurons upon 2 h of OGD (Figure 1b). The results of reverse transcription-polymerase chain reaction (RT-PCR) and statistical analysis demonstrated that 14-3-3 $\gamma$  transcriptions

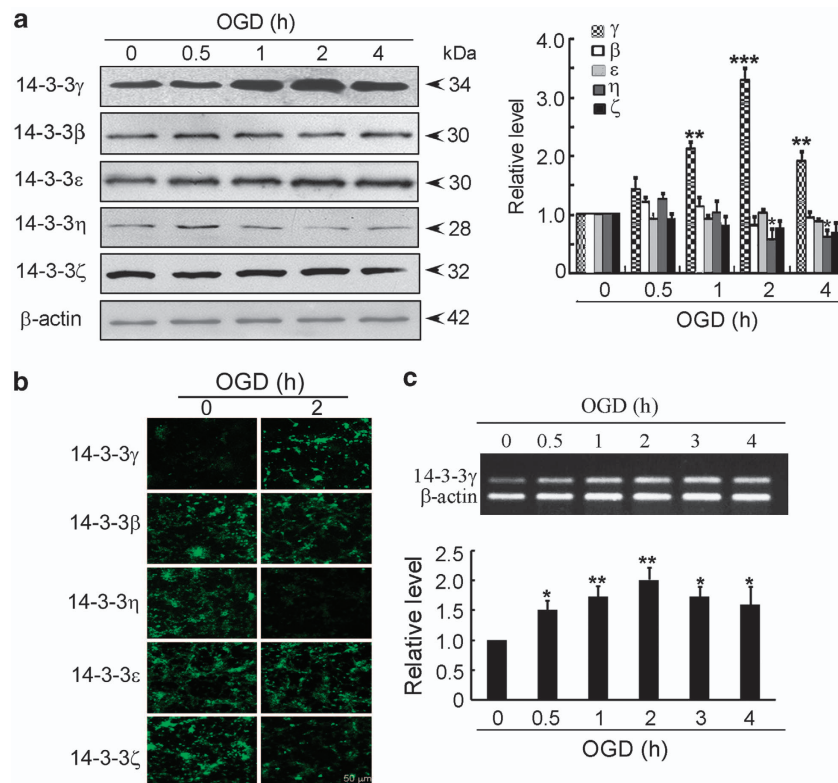


**Figure 1** 14-3-3 $\gamma$  is selectively upregulated in primary cultures of cerebral cortical neurons upon OGD. Primary cultures of rat cerebral cortical neurons at 7 DIV were incubated with OGD media in an anaerobic chamber (0.1% O<sub>2</sub>) for the indicated time and were then subjected to different assays. (a) Representative western blot results and statistical analysis of 14-3-3 isoforms ( $\beta$ ,  $\epsilon$ ,  $\eta$ ,  $\gamma$  and  $\zeta$ ).  $\beta$ -Actin was used as the internal control. The relative level represented the ratio of 14-3-3/ $\beta$ -actin. \*\* $P$  < 0.01, \*\*\* $P$  < 0.001 versus 0 h ( $n$  = 3). (b) Representative fluorescent immunostaining results of 14-3-3 $\beta$ ,  $\epsilon$ ,  $\eta$ ,  $\gamma$  and  $\zeta$  in cultured neurons upon 2 h of OGD. (c) Representative RT-PCR results and statistical analysis of 14-3-3 $\gamma$  in cultured neurons upon OGD.  $\beta$ -actin was amplified simultaneously with 14-3-3 $\gamma$  as the internal control. The relative level represents the ratio of 14-3-3/ $\beta$ -actin. \* $P$  < 0.05, \*\* $P$  < 0.01 versus 0 h ( $n$  = 3)

were significantly increased in primary cortical neurons upon 0.5, 1, 2, 3 and 4 h of OGD (Figure 1c).

The OGD responses of 14-3-3 isoforms were then investigated in animal ischemic stroke rats with complexity of the cellular components and ischemic pathology in the brain. On subjecting to 24 h of permanent middle cerebral artery occlusion (pMCAo), the ischemic infarct was prominent (white area in the brain slice, triphenyltetrazolium chloride (TTC) staining, Figure 2a). Brain cells in the penumbra area of the ipsilateral cortex (Ipsi, indicated by the box, Figure 2a) of the 1 h-pMCAo rat were injured moderately and could elicit protective responses and were used for analyzing 14-3-3

expression. Fluorescent double immunostaining confirmed that 14-3-3 $\gamma$  was expressed in cortical neurons (specific with NeuN) in the Ipsi of rats with 1 h of pMCAo (Figure 2b). Results of histochemical analysis clearly showed that 14-3-3 $\gamma$  (Figure 2c) but not 14-3-3 $\beta$ ,  $\epsilon$ ,  $\eta$  and  $\zeta$  (Supplementary Figure 2) was evidently increased in cortical neurons in the Ipsi as compared with its contralateral counterpart (Contra) in rats with 1 h of pMCAo. Statistical analysis demonstrated that the relative level of 14-3-3 $\gamma$  but not 14-3-3 $\beta$ ,  $\epsilon$ ,  $\eta$  and  $\zeta$  was significantly increased in the Ipsi as compared with the Contra in rats with 1 h of pMCAo (Figure 2d). Consistently, results of quantitative polymerase chain reaction (qPCR) (Figure 2e)

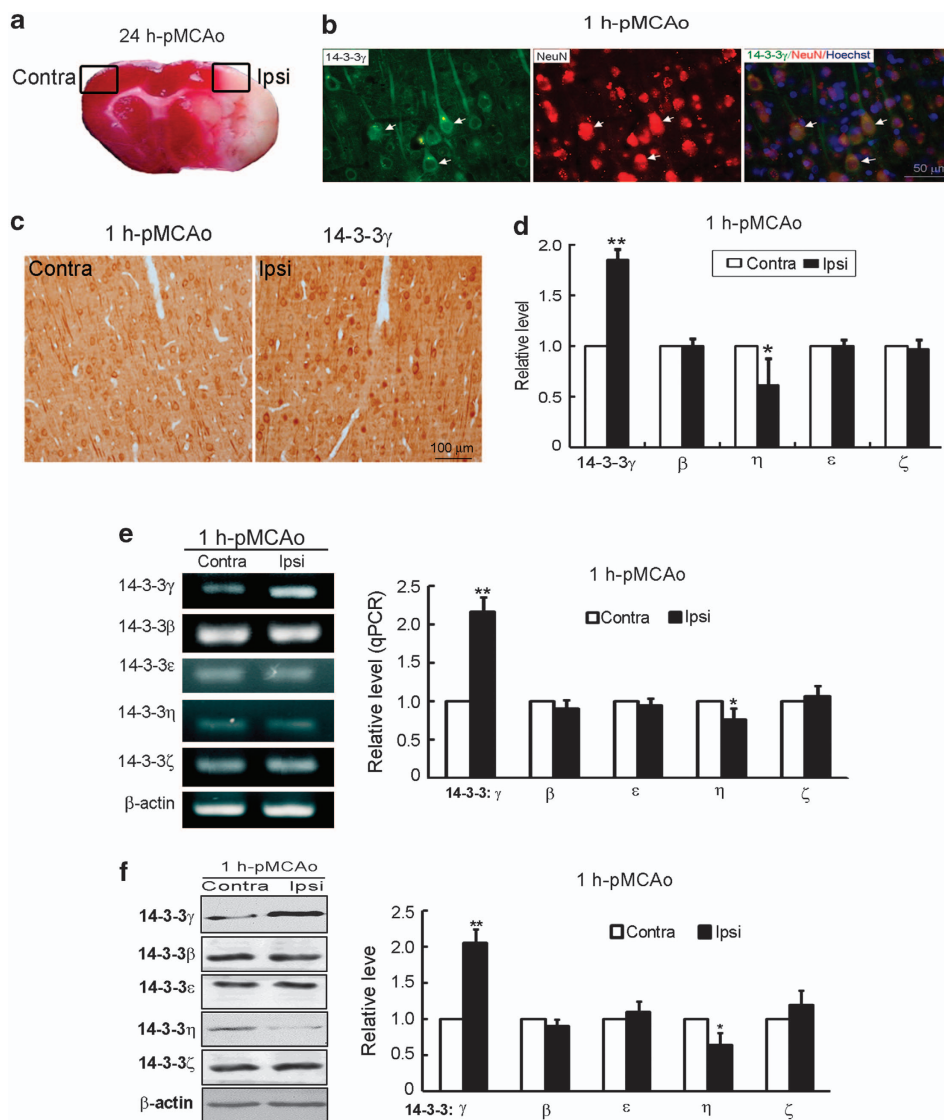


**Figure 2** 14-3-3 $\gamma$  is selectively upregulated in cerebral cortical neurons in 1 h-pMCAo rats. (a) Representative ischemic rat brain slice after TTC staining showing the ipsilateral penumbra area (Ipsi, indicated by the black box) and its Contra for 14-3-3 isoform measurements. (b) Representative micrographs of double-fluorescent immunostaining showing the expression of 14-3-3 $\gamma$  in cerebral cortical neurons in the Ipsi of 1 h-pMCAo. NeuN is a marker of neurons. Arrows indicate neurons co-expressing 14-3-3 $\gamma$  and NeuN. (c) Representative micrographs of IHC showing the elevation of 14-3-3 $\gamma$  in the Ipsi of 1 h-pMCAo rat. (d) Statistical analysis of relative expression levels of 14-3-3 isoforms in the Ipsi of 1 h-pMCAo rats. The average intensity of 14-3-3 isoform was measured from more than 100 neurons in each IHC micrograph by using Plus software. The relative expression level of 14-3-3 isoform in the Ipsi was compared with that of Contra. \* $P < 0.05$  versus its Contra ( $n = 7$ ). (e) Representative results of RT-PCR (left panel) and statistical analysis of qPCR (right panel) of 14-3-3 isoforms in the Contra and Ipsi of 1 h-pMCAo rats. Relative 14-3-3 level was normalized to that of  $\beta$ -actin. \* $P < 0.05$ , \*\* $P < 0.01$  versus Contra ( $n = 6$ /group). (f) Representative western blot results (left panel) and statistical analysis (right panel) of 14-3-3 isoforms in the Contra and Ipsi of 1 h-pMCAo rats. Relative 14-3-3 level was normalized to that of  $\beta$ -actin. \* $P < 0.05$ , \*\* $P < 0.01$  versus Contra ( $n = 6$ /group)

demonstrated that only 14-3-3 $\gamma$  mRNA but not 14-3-3 $\beta$ ,  $\epsilon$ ,  $\eta$  and  $\zeta$  mRNA was selectively upregulated in the Ipsi as compared with the Contra in rats with 1 h of pMCAo. Further, results of western blot analysis demonstrated the 14-3-3 $\gamma$  but not 14-3-3 $\beta$ ,  $\epsilon$ ,  $\eta$  and  $\zeta$  was significantly increased in the Ipsi of 1 h-pMCAo rats as compared with the Contra (Figure 2f). These *in vitro* and *in vivo* data together demonstrated that ischemia selectively upregulated only the  $\gamma$ -isoform of 14-3-3 in cerebral cortical neurons.

**14-3-3 $\gamma$  protects cortical neurons from OGD-induced cell death.** Since only 14-3-3 $\gamma$  was upregulated, we focused on investigating the functional role of this isoform in OGD-treated neurons. Results of fluorescent double-immunostaining showed that 14-3-3 $\gamma$  was elevated in surviving neurons (indicated by conclave arrowheads, Figure 3a) but nearly undetectable in dying neurons (with elevated cleaved caspase-3 and highly condensed nuclei, indicated by arrows, Figure 3a) subjected to 6 h of OGD. In addition, 14-3-3 $\gamma$  was elevated in neurons that survived 24 h post 2 h OGD (indicated by conclave arrowheads, Supplementary Figure 3) but evidently decreased in caspase 3-activated (upper panels, indicated by arrows) or TUNEL-positive (lower panels, indicated by arrows, Supplementary Figure 3) neurons. This evidence supported a positive correlation between 14-3-3 $\gamma$  levels and the survival of OGD-treated neurons. To investigate the causative effects of 14-3-3 $\gamma$  on the survival or death of OGD-treated neurons, 14-3-3 $\gamma$  was overexpressed or knocked down by RNA interfering technique. The average transfection efficiency in primary cortical neurons by using the nucleofector was around 65% (Figure 3b). Overexpression of 14-3-3 $\gamma$ -shRNA (short hairpin RNA) plasmids for 3 days reduced 14-3-3 $\gamma$  to  $\sim$ 25% of that in scrambled negative control (N-con) in primary cortical neurons, verifying the successful knockdown of endogenous 14-3-3 $\gamma$  (Figure 3c). 14-3-3 $\gamma$  knockdown in primary cortical neurons at 7 DIV induced significant cell death (0 h, 13.3% *versus* 9.7% in N-con, Figure 3d) under normal culture conditions as measured by PI staining, suggesting that endogenous 14-3-3 $\gamma$  alone was important for the survival of cortical neurons. Moreover, knockdown of 14-3-3 $\gamma$  significantly exacerbated cell death in primary cortical neurons subjected to 1 h (20.8% *versus* 15.1% in N-con) and 3 h (33.8% *versus* 27.3% in N-con) of OGD (Figure 3d). On the contrary, enhancing 14-3-3 $\gamma$  by ectopic overexpression significantly reduced cell death in primary cortical neurons subjected to 4 h (22% *versus* 31% in con, Figure 3e) and 6 h (47% *versus* 64% in con, Figure 3e) of OGD. Further, we compared the protective effect of each 14-3-3 isoform ( $\beta$ ,  $\epsilon$ ,  $\eta$ ,  $\gamma$ ,  $\sigma$ ,  $\tau$  and  $\zeta$ ) in OGD-treated neuroblastoma N2a cells, and the results of LDH and MTT assays demonstrated that the 14-3-3 $\gamma$  exerted the maximal protection in N2a cells upon 2 h of OGD (Supplementary Figure 4). Taken together, 14-3-3 $\gamma$  was an important intrinsic protective factor in cortical neurons during OGD.

**14-3-3 $\gamma$  binds specifically to more p- $\beta$ -catenin Ser37 in the nuclei of ischemic neurons.** After demonstrating the protective role of 14-3-3 $\gamma$  in OGD-treated neurons, we further investigated the underlying mechanisms. It is well known

that 14-3-3 proteins function by interacting with other proteins.<sup>14,15</sup> In primary cortical neurons, inhibiting the interactions of 14-3-3 proteins with their client proteins by overexpressing the specific 14-3-3 blocking peptide Difo-pein<sup>11</sup> induced severe cell death in cortical neurons at 3 DIV (day *in vitro*) under normal conditions (Figure 4a) and significantly aggravated the death of cortical neurons at 2 DIV upon 2 or 4 h of OGD as measured by PI staining (Figure 4b), supporting that 14-3-3 proteins exert their protection via protein-protein interactions. We have previously reported that 14-3-3 $\gamma$  prevented primary cortical astrocytes from OGD-induced cell death by binding to more p-Bad Ser112 in the cytoplasm.<sup>20</sup> In primary cortical neurons, results of co-immunoprecipitation (co-IP) showed that 14-3-3 $\gamma$  also bound to p-Bad Ser112 but their interactions decreased prominently upon 2 and 4 h of OGD incubation (Figure 4c). We then examined the interaction of 14-3-3 $\gamma$  with other well-known pro-apoptotic proteins such as Bax, Ask-1 and p53. Results of co-IP showed that 14-3-3 $\gamma$  bound to little Bax, p-Ask-1 Ser966 (Figure 4c) and p-p53 Ser315 (Figure 4d) in primary cultured cortical neurons under normal or OGD incubation. Therefore, it is unlikely that 14-3-3 $\gamma$  protected ischemic neurons via binding to these well-known 14-3-3 client proteins in the cytoplasm to suppress their apoptotic effects directly.

14-3-3 $\gamma$  has been reported to be presented in the nuclei of OGD-treated astrocytes.<sup>22</sup> Recently, a function of 14-3-3 in gene regulation was also reported.<sup>23</sup> Thus, we investigated the interaction of 14-3-3 $\gamma$  with  $\beta$ -catenin, an important transcriptional factor involved in cell death or survival. Results of co-IP showed a prominent increase of 14-3-3 $\gamma$ -p- $\beta$ -catenin Ser37 interaction in primary cortical neurons upon 2 and 4 h of OGD incubation (Figure 4d). Further, fluorescence resonance energy transfer (FRET) assay demonstrated that endogenous 14-3-3 $\gamma$  bound directly to more p- $\beta$ -catenin Ser37 in OGD-treated neurons. In control (0 h) and OGD-treated (2 h) neurons (indicated by arrows, Figure 4e), bleaching of p- $\beta$ -catenin Ser37 fluorescence of the whole neuron (red color in the lower panels of Figure 4e, served as the acceptor in FRET assay) evidently enhanced the fluorescent intensity of 14-3-3 $\gamma$  of the same neuron (green color in the upper panels of Figure 4e, served as the donor). Statistical analysis demonstrated that the percentage of 14-3-3 $\gamma$ /p- $\beta$ -catenin Ser37 FRET-positive cells (69% at 2 h OGD *versus* 40% at 0 h, Figure 4f) and the mean 14-3-3 $\gamma$ /p- $\beta$ -catenin Ser37 FRET efficiency (21% at 2 h OGD *versus* 10% at 0 h, Figure 4g) were significantly increased in OGD-treated neurons, while the mean 14-3-3 $\gamma$ /Bax FRET efficiency was not altered (Figure 4g). This evidence strongly suggested that 14-3-3 $\gamma$  protected ischemic neurons by direct binding to more p- $\beta$ -catenin Ser37.

Consistent with the increase of 14-3-3 $\gamma$ /p- $\beta$ -catenin Ser37 binding, results of western blot demonstrated that p- $\beta$ -catenin Ser37 was prominently increased in primary cortical neurons upon 1, 2, 3 and 4 h of OGD (Figure 5a). Results of fluorescent immunostaining showed an evident increase of p- $\beta$ -catenin Ser37 but not p- $\beta$ -catenin Ser45 in cultured cortical neurons upon 2 h of OGD (Figure 5b), suggesting that  $\beta$ -catenin was phosphorylated mainly at Ser37 in cortical neurons upon OGD. In the Contra of rat brains, p- $\beta$ -catenin Ser37 was

homogenously distributed in cortical neurons as compared with the cytoplasmic distribution of 14-3-3 $\gamma$  (Figure 5c). On subjecting to 1 h of pMCAo, both p- $\beta$ -catenin Ser37 and 14-3-3 $\gamma$  were accumulated in the nuclei of cortical neurons<sup>24</sup> in the Ipsi (indicated by arrows, Figure 5c). Further, results of fluorescent double-immunostaining clearly showed that p- $\beta$ -catenin Ser37 and 14-3-3 $\gamma$  were co-translocated into the nuclei of same neuron upon 2 h of OGD (Figure 5d).

Therefore, OGD promoted 14-3-3 $\gamma$  and p- $\beta$ -catenin Ser37 binding in the nuclei of cortical neurons.

**14-3-3 $\gamma$  protects ischemic neurons by downregulating Bax.** The binding of 14-3-3 $\gamma$  and p- $\beta$ -catenin Ser37 in the nuclei suggests that 14-3-3 $\gamma$  may regulate gene expression via p- $\beta$ -catenin Ser37 in ischemic neurons. Therefore, we further examined the regulatory effects of 14-3-3 $\gamma$  on the

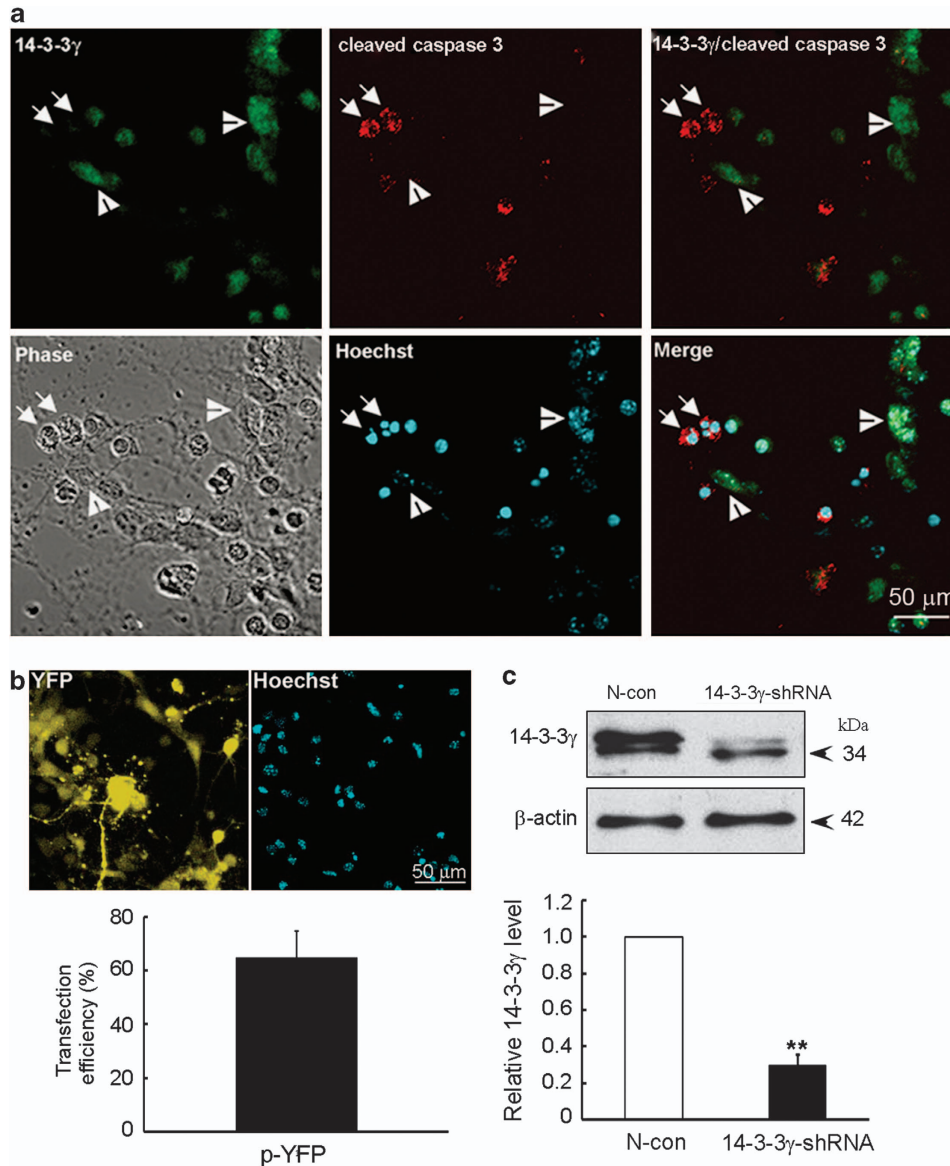


**Figure 3** 14-3-3 $\gamma$  promotes the survival of cortical neurons and protects them from OGD-induced death. (a) Representative micrographs of double-fluorescent immunostaining showing the segregation of endogenous 14-3-3 $\gamma$  and cleaved caspase-3 or nuclear condensation in cultured neurons upon 6 h of OGD. Conclaved arrowheads indicated survived neurons while arrows indicated dead neurons. (b) Representative fluorescent micrographs and statistical analysis showing the transfection efficiency in cultured cortical neurons by using the nuclear-transfection method. Freshly isolated cortical neurons were subjected to nuclear transfection with p-EYFP-C1 plasmids. The transfection efficiency (% of YFP<sup>+</sup>-cells) was calculated 7 days after transfection. (c) Representative western blot results and statistical analysis showing the effect of 14-3-3 $\gamma$  knockdown in cultured neurons by nuclear-transfecting 14-3-3 $\gamma$ -shRNA or N-con. Western blot analysis was performed 7 days after transfection. Relative 14-3-3 $\gamma$ / $\beta$ -actin level was compared with that of N-con (scramble control shRNA). \*\* $P < 0.01$  versus N-con ( $n = 3$ ). (d) Representative fluorescent micrographs and statistical analysis showing the effect of 14-3-3 $\gamma$  knockdown on OGD-induced cell death in cultured cortical neurons. Transfected neurons at 7 DIV were subjected to 0, 1 and 3 h of OGD. Dead cells were visualized by PI staining. The percentage of cell death was estimated by counting over 200 cells from at least six different fields. \*\* $P < 0.01$  versus corresponding N-con ( $n = 3$ ). (e) Representative fluorescent micrographs and statistical analysis showing the effect of 14-3-3 $\gamma$  overexpression on OGD-induced cell death in cultured cortical neurons. Isolated cortical neurons were nuclear-transfected with pcDNA-14-3-3 $\gamma$  or pcDNA. Transfected neurons at 7 DIV were subjected to 0, 4 or 6 h of OGD. Dead cells were visualized by PI staining. \*\* $P < 0.01$  versus corresponding control ( $n = 3$ )

expression of Bcl-2 families as they are gatekeepers controlling mitochondria-mediated cell death. Results of qPCR demonstrated that 14-3-3 $\gamma$  overexpression significantly reduced Bax mRNA, but did not alter the transcripts of other Bcl-2 members such as Bcl-2, Bad, Bcl-x<sub>L</sub> and MCL-1 in cultured neurons at 7 DIV (Figure 6a). Results of western blot analysis demonstrated that doubling 14-3-3 $\gamma$  amounts by ectopic overexpression reduced 70% of endogenous Bax as compared with untreated (–) and pcDNA controls in cultured neurons at 7 DIV (Figure 6b). Consistently, knockdown of endogenous 14-3-3 $\gamma$  by overexpressing 14-3-3 $\gamma$ -shRNA for 3 days significantly reduced endogenous 14-3-3 $\gamma$  and increased Bax as compared with the N-con in N2a cells (Figure 6c). Further, the results of western blot showed that 14-3-3 $\gamma$  had a maximal effect on reducing Bax as compared with the other 14-3-3 isoforms in N2a cells (Supplementary Figure 5a). These data together demonstrated a critical role of 14-3-3 $\gamma$  in reducing Bax. Overexpressing Bax in N2a cells caused ~80% of cell death in GFP + Bax co-transfected cells as measured by GFP expression level under normal culture conditions (indicated by arrows, Supplementary Figure 5b), supporting a critical role of Bax in inducing cell death. In primary cortical neurons, Bax was upregulated prominently upon 4 and 6 h of OGD (Figure 7a). Consistently, 2 h of pMCAo induced Bax in cortical neurons in the Ipsi of rat brain (Figure 7b). Therefore, the elevation of Bax was a key damaging factor in OGD/ischemic neurons. We then analyzed the relationship between 14-3-3 $\gamma$  and Bax levels in

ischemic neurons *in vivo*. Results of fluorescent double-immunostaining clearly showed that 14-3-3 $\gamma$  elevation in the nuclei (indicated by arrows, Ipsi, Figure 7c) was segregated from Bax elevation in cortical neurons in the Ipsi of rats subjected to 6 h of pMCAo, consistent with the inhibitory effect of 14-3-3 $\gamma$  on Bax expression. Finally, we verified the regulatory role of 14-3-3 $\gamma$  in Bax expression in OGD-treated neurons. Knockdown of 14-3-3 $\gamma$  significantly increased Bax and cleaved caspase-3 in cultured cortical neurons upon 4 h of OGD (Figure 7d). These data together demonstrated that 14-3-3 $\gamma$  prevented ischemic death of cortical neurons by reducing Bax.

**14-3-3 $\gamma$  suppresses Bax expression via a p- $\beta$ -catenin Ser37-mediated mechanism.** After the key downstream target of 14-3-3's protection was identified, we then investigated whether 14-3-3 $\gamma$  reduced Bax and cell death via p- $\beta$ -catenin Ser37 interaction or not. Overexpression of wild type  $\beta$ -catenin ( $\beta$ -catenin<sup>WT</sup>) significantly increased the death of cultured cortical neurons upon 2 h of OGD, while abolishing  $\beta$ -catenin phosphorylation at Ser37 by overexpressing  $\beta$ -catenin<sup>S37A</sup> completely reversed  $\beta$ -catenin<sup>WT</sup> enhanced cell death as measured by PI staining (Figure 8a). This evidence demonstrated that p- $\beta$ -catenin Ser37 itself was a cell death component of cortical neurons upon OGD. Results of western blot demonstrated that overexpressing  $\beta$ -catenin<sup>S37A</sup> significantly reduced Bax in cultured neurons as compared with  $\beta$ -catenin<sup>WT</sup> (Figure 8b). In ischemic rat

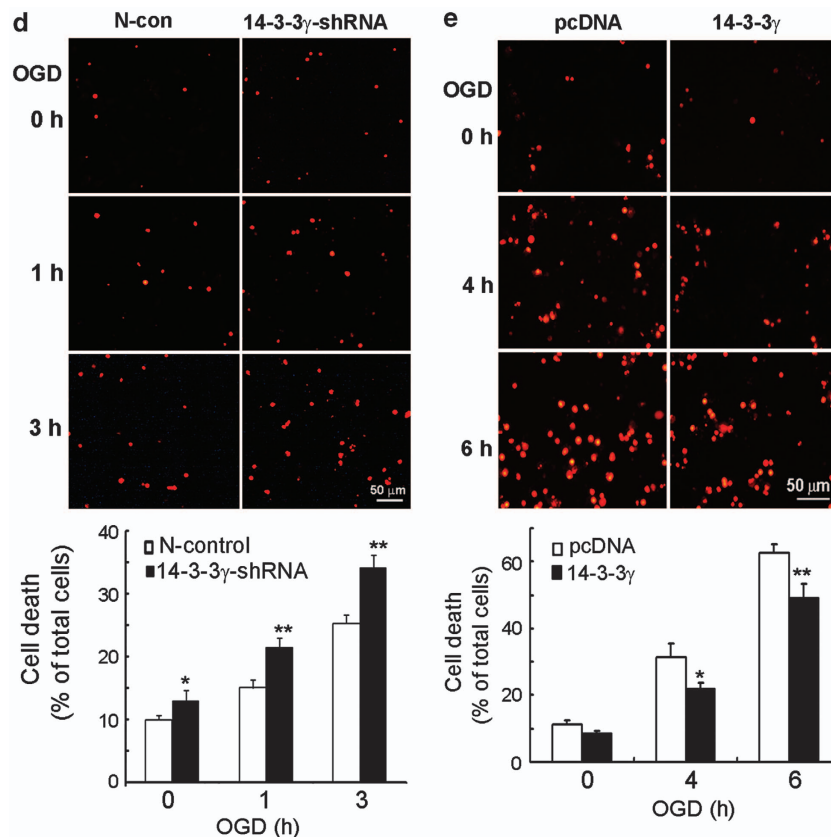


**Figure 3** (Continued)

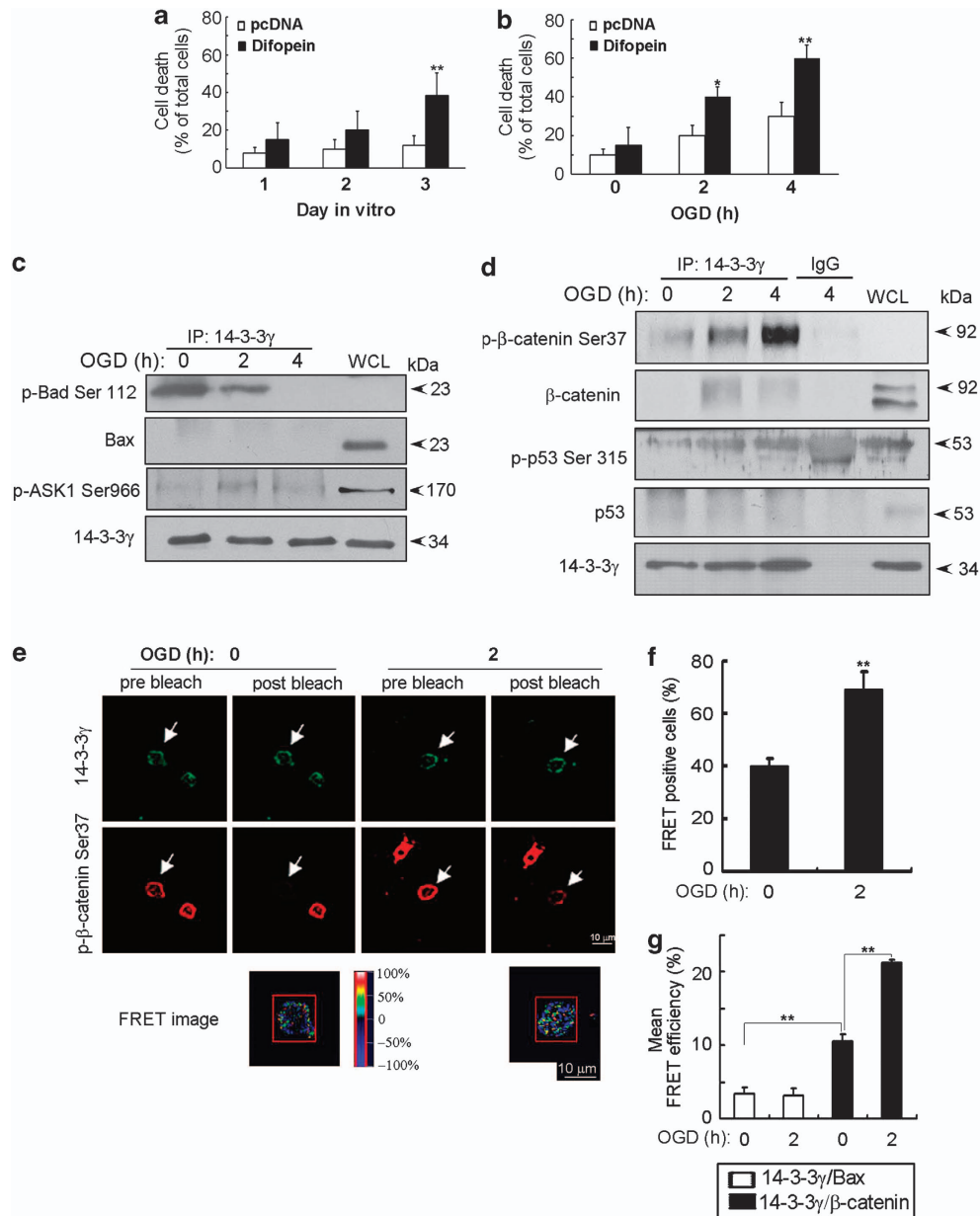


**Figure 4** 14-3-3 $\gamma$  binds specifically to more p- $\beta$ -catenin Ser37 in OGD-treated neurons. (a) Effect of Difopein overexpression on cell death in cultured neurons. Cultured cortical neurons were nuclear-transfected with pcDNA-Difopein or pcDNA plasmids for 1, 2 or 3 days and were subjected to cell death analysis by PI staining.  $**P < 0.01$  versus corresponding pcDNA ( $n = 3$ ). (b) Effect of Difopein overexpression on cell death in cultured neurons upon OGD. After 2 days of nuclear transfection, cultured neurons were subjected to 0, 2 or 4 h of OGD. Cell death was analyzed by PI staining.  $*P < 0.01$ ,  $**P < 0.01$  versus corresponding pcDNA ( $n = 3$ ). (c) Representative results of co-IP showing the interaction of 14-3-3 $\gamma$  with p-Bad Ser112, p-ASK-1 Ser966 and Bax in cultured neurons upon OGD. Cultured neurons at 7 DIV were subjected to 0, 2 or 4 h of OGD. Mouse anti-14-3-3 $\gamma$  antibodies were used for IP. Rabbit anti-p-Bad Ser112, p-ASK-1 Ser966, Bax or 14-3-3 $\gamma$  antibodies were used for western blot. WCL, whole cell lysate. (d) Representative results of co-IP showing the interactions of 14-3-3 $\gamma$  with p- $\beta$ -catenin Ser37,  $\beta$ -catenin, p-p53 Ser315 and p53 in cultured neurons upon OGD. Normal mouse IgG was used as a negative control of IP. (e) Representative fluorescent micrographs of FRET showing the direct 14-3-3 $\gamma$ /p- $\beta$ -catenin Ser37 binding in cultured neurons upon OGD. Cultured neurons at seven DIV were subjected to 0 or 2 h of OGD and co-stained with anti-14-3-3 $\gamma$  and p- $\beta$ -catenin Ser37 antibodies. p- $\beta$ -catenin Ser37 (red, served as FRET acceptor) of the whole cell body of neurons was bleached and the fluorescence of 14-3-3 $\gamma$  (green, served as FRET donor) was recorded simultaneously before and after acceptor bleaching. The FRET images were produced by using the FRET software. Arrows indicate bleached neurons and red boxes in FRET images indicate the cell body of bleaching. (f) Statistical analysis of FRET-positive cells in cultured neurons upon 2 h of OGD. FRET-positive cells were defined by an increase of 20% or more in the fluorescent intensity of the donor protein after acceptor bleaching.  $*P < 0.05$  versus 0 h ( $n = 100$  cells/group). (g) Statistical analysis of FRET efficiency of 14-3-3 $\gamma$ /p- $\beta$ -catenin Ser37 or 14-3-3 $\gamma$ /Bax pairs in cultured neuron upon 2 h of OGD. Mean FRET efficiency represents the average increase of the fluorescent intensity of the donor protein after acceptor bleaching.  $**P < 0.01$  versus 0 h of corresponding protein pairs ( $n = 50$  cells/group)

brain, results of double-fluorescent immunostaining showed that higher nuclear  $\beta$ -catenin Ser37 levels were correlated well with higher Bax levels in cortical neurons (indicated by

arrows, Figure 8c) in the Ipsi of rats subjected to 2 h of pMCAo. The coefficient ( $R^2$ ) of p- $\beta$ -catenin Ser37 and Bax fluorescent intensities in ischemic neurons was 0.86

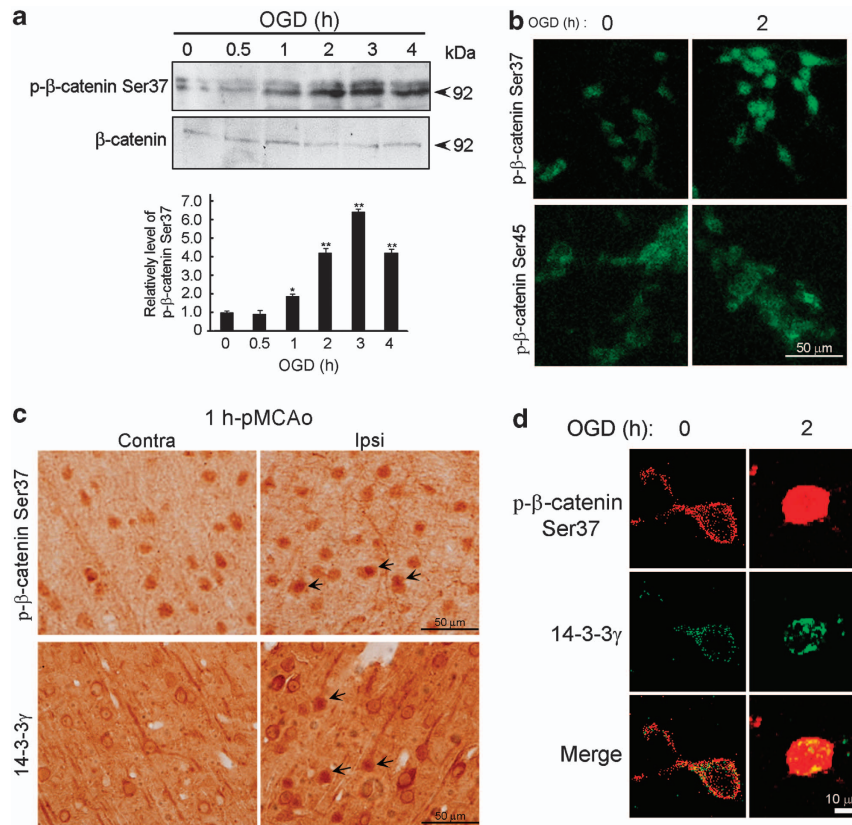


**Figure 5** p- $\beta$ -catenin Ser37 is elevated and co-translocated in the nucleus with 14-3-3 $\gamma$  in OGD/ischemic neurons. (a) Representative western blot results and statistical analysis showing p- $\beta$ -catenin Ser37 levels in cultured cortical neurons upon OGD. Relative p- $\beta$ -catenin Ser37 level was normalized to the corresponding total  $\beta$ -catenin level. \* $P < 0.05$ , \*\* $P < 0.01$  versus 0 h ( $n = 3$ ). (b) Representative fluorescent micrographs showing the expression of p- $\beta$ -catenin Ser37 and p- $\beta$ -catenin Ser45 in cultured neurons upon 2 h of OGD. (c) Representative micrographs of IHC showing the existence of p- $\beta$ -catenin Ser37 and 14-3-3 $\gamma$  in the nuclei of cortical neurons in the Ipsi of 1 h-pMCAo rats. Arrows indicated ischemic cortical neurons with nuclear p- $\beta$ -catenin Ser37 and 14-3-3 $\gamma$ . (d) Representative micrographs of double-fluorescent immunostaining showing the co-translocation of endogenous p- $\beta$ -catenin Ser37 and 14-3-3 $\gamma$  into the nucleus of cultured neuron upon 2 h of OGD

(Figure 8d). These data together demonstrated a critical role of p- $\beta$ -catenin Ser37 in reducing Bax.

Finally, we demonstrated that 14-3-3 $\gamma$  overexpression significantly reduced  $\beta$ -catenin<sup>WT</sup>-induced cell death in cultured cortical neurons upon 2 h of OGD as measured by PI staining (Figure 8e). Consistently,  $\beta$ -catenin<sup>WT</sup>-induced Bax upregulation was completely abolished by co-overexpressing 14-3-3 $\gamma$  in cortical neurons upon 2 h of OGD (Figure 8f). Taken together, 14-3-3 $\gamma$  reduced the cell death of ischemic neurons by suppressing p- $\beta$ -catenin Ser37/Bax signaling.

## Discussion

In the present study, we demonstrated that 14-3-3 $\gamma$  was an important early ischemia-inducible protective factor in cerebral cortical neurons. Further, we identified a neuronal-specific protective mechanism, that is, 14-3-3 $\gamma$ /p- $\beta$ -catenin Ser37/Bax axis in ischemic neurons, dependent on 14-3-3 $\gamma$ /p- $\beta$ -catenin Ser37 interactions in the nucleus.

We tested whether 14-3-3 $\gamma$  was an intrinsic survival factor in neurons. In pure cultured cerebral cortical neurons and cortical neurons *in vivo*, only the  $\gamma$  but not any other isoform of 14-3-3 could be upregulated by OGD or pMCAo. We have

previously demonstrated that 14-3-3 $\gamma$  is selectively upregulated in pure cultured cerebral cortical astrocytes.<sup>20</sup> These evidences suggest that the ischemic response of 14-3-3 $\gamma$  is well conserved in different kinds of brain cells. 14-3-3 $\gamma$  elevation was prominent after 1 and 3 h of pMCAo but not 6 h of pMCAo (Supplementary Figure 6a), suggesting that 14-3-3 $\gamma$  was an early ischemia-responsive gene. This property was further supported by using the decapitated ischemic model, in which 14-3-3 $\gamma$  elevation in the cerebral cortices of rats was detected within 15 min after decapitation (Supplementary Figure 6b). Hypoxia (0.1% O<sub>2</sub>) (Supplementary Figure 6c) or glucose deprivation (Supplementary Figure 6d) alone did not elevate 14-3-3 $\gamma$  until 6 h of treatment in cultured neurons, suggesting a synergistic effect of hypoxia and glucose deprivation on 14-3-3 $\gamma$  induction during OGD. Among all 14-3-3 isoforms, 14-3-3 $\gamma$  exerted a greater protective effect in neuronal cells upon OGD. Reducing endogenous 14-3-3 $\gamma$  exacerbated neuronal death, while increasing 14-3-3 $\gamma$  reduced neuronal cell. Thus, we concluded that 14-3-3 $\gamma$  was an early ischemia-inducible protective factor. Our findings narrowed down the protection of 14-3-3 families to a single isoform, making it more practical by targeting 14-3-3 for stroke treatment. Since 14-3-3 $\gamma$  was the only isoform induced by OGD/ischemia, we speculated that ischemic pre-conditioning

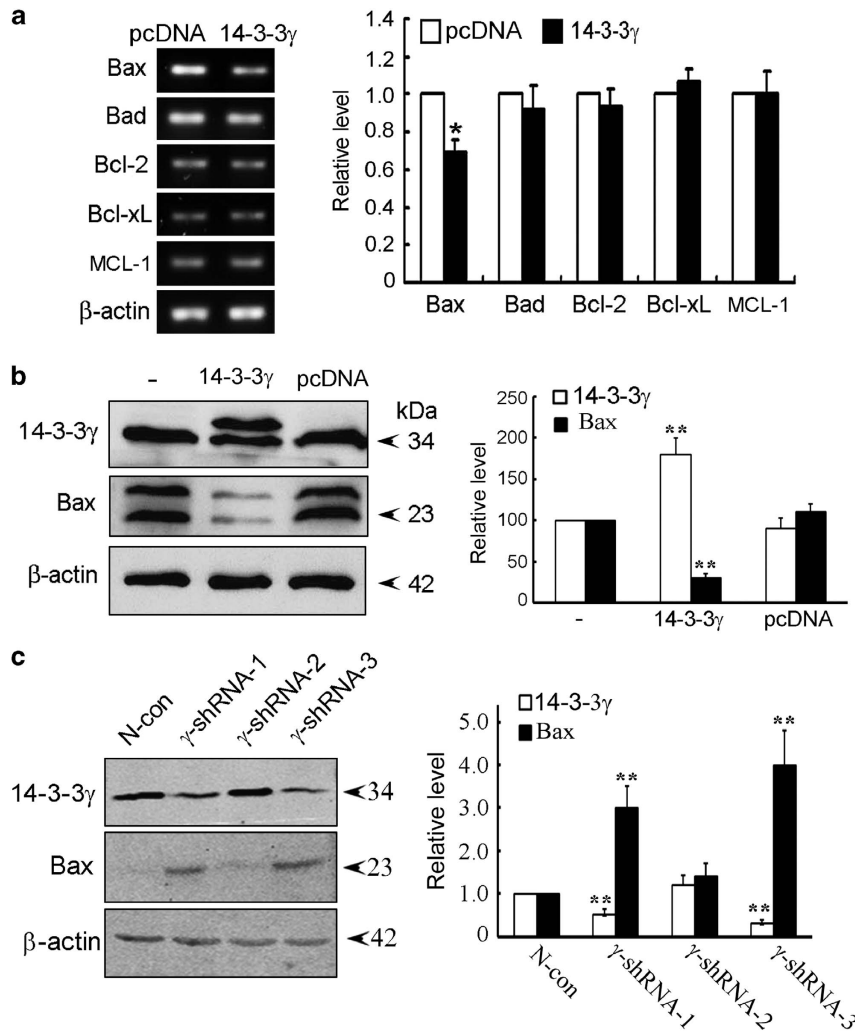


**Figure 6** 14-3-3 $\gamma$  is a negative regulator of Bax expression in neurons. (a) Representative qPCR results and statistical analysis showing the effects of 14-3-3 $\gamma$  overexpression on the expression of Bcl-2 members in cultured neurons. Cultured neurons were nuclear-transfected with pcDNA-14-3-3 $\gamma$  or pcDNA for 7 days. The expression levels of Bad, Bcl-2, Bax, Bcl-x<sub>L</sub> and MCL-1 mRNA were measured by qPCR.  $\beta$ -actin served as the internal control. \*\* $P < 0.01$  versus vec ( $n = 3$ ). (b) Representative western blot results and statistical analysis showing the effect of 14-3-3 $\gamma$  overexpression on Bax expression in cultured neurons at 7 DIV. -, untransfected control.  $\beta$ -actin served as the internal control. \*\* $P < 0.01$  versus vec ( $n = 3$ ). (c) Representative western blot results and statistical analysis showing the effect of 14-3-3 $\gamma$  knockdown on Bax expression in N2a cells. \*\* $P < 0.01$  versus corresponding N-control ( $n = 3$ )

might exert a protection by inducing 14-3-3 $\gamma$ . To test this possibility, we pretreated mice with CoCl<sub>2</sub>, a well-known chemical ischemic pre-conditioning inducer,<sup>25,26</sup> and found that CoCl<sub>2</sub> indeed elevated only the  $\gamma$  isoform of 14-3-3 in mouse cerebral cortex (Supplementary Figure 7). This evidence strongly suggested that inducing 14-3-3 $\gamma$  by chemical compounds in the brain is a feasible strategy in order to elongate the therapeutic time window for thrombolytic therapy after ischemic stroke.

14-3-3 proteins could prevent cell death by binding to different pro-apoptotic proteins.<sup>27,28</sup> Under normal conditions, 14-3-3 $\gamma$  was distributed predominantly in the cytoplasm and bound mainly to p-Bad Ser112 in cortical neurons. This interaction is well known for the antiapoptotic role of 14-3-3 proteins.<sup>29</sup> Upon OGD, 14-3-3 $\gamma$  bound to less p-Bad Ser112 and entered into the nucleus, where it bound to increasing amounts of p- $\beta$ -catenin Ser37.  $\beta$ -Catenin is a critical transcriptional factor regulating cell death and

survival and its regulatory mechanism is not fully understood.<sup>30–32</sup> p- $\beta$ -catenin Ser37 was distributed predominantly in the nucleus of cerebral cortical neurons upon ischemia,<sup>24</sup> suggesting that p- $\beta$ -catenin Ser37 itself might be an important transcriptional factor. The direct binding of 14-3-3 $\gamma$  with p- $\beta$ -catenin Ser37 in the nucleus might suppress the transcriptional function of p- $\beta$ -catenin Ser37 in the nucleus and Bax might be an important target of p- $\beta$ -catenin Ser37. Bax is a key ischemia-inducible cell death factor<sup>33–35</sup> and its regulation remains not fully understood. 14-3-3 $\gamma$  reduced Bax but did not bind to it directly in cortical neurons. Abolishing  $\beta$ -catenin phosphorylation at Ser37 alone by point mutation reduced Bax expression and enhanced neuronal survival during OGD, resembling the effects of 14-3-3 $\gamma$  overexpression on reducing Bax and OGD-induced cell death. Therefore, we proposed that 14-3-3 $\gamma$  suppressed Bax via p- $\beta$ -catenin Ser37 interaction in neurons upon OGD or ischemia.

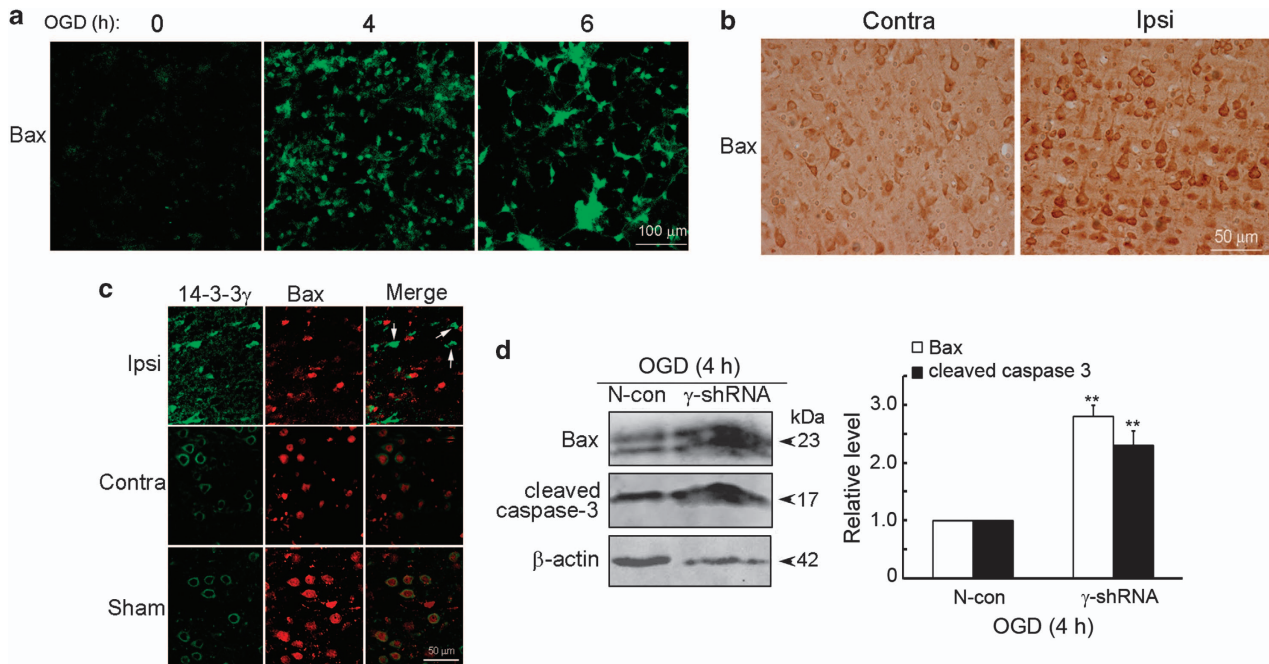


**Figure 7** 14-3-3 $\gamma$  suppresses OGD/ischemia-induced Bax in cortical neurons *in vitro* and *in vivo*. (a) Representative fluorescent micrographs showing the expression of Bax in cultured neurons upon 4 or 6 h of OGD. (b) Representative micrographs of IHC showing the expression of Bax in cortical neurons of the Contra and Ipsi of rats subjected to 1 h of pMCAo. (c) Representative micrographs of double-fluorescent immunostaining showing the segregation of 14-3-3 $\gamma$  and Bax expression in the Ipsi of rats subjected to 6 h of pMCAo. (d) Representative Western blot results and statistical analysis showing the effects of 14-3-3 $\gamma$  knockdown on Bax and cleaved caspase-3 levels in cultured cortical neurons upon 4 h of OGD. \*\* $P < 0.01$  versus N-con ( $n = 3$ )

It is reported that the binding of 14-3-3 $\zeta$  to p- $\beta$ -catenin Ser37 might reduce  $\beta$ -catenin degradation and thus increases total  $\beta$ -catenin to reduce cell death.<sup>36</sup> In OGD-treated neurons, however, the elevation of total  $\beta$ -catenin was not detected.<sup>37</sup> Consistently, total  $\beta$ -catenin was not increased by 14-3-3 $\gamma$  overexpression. Moreover, overexpression of  $\beta$ -catenin<sup>WT</sup> enhanced Bax and cell death in cortical neurons upon OGD. These data suggested that 14-3-3 $\gamma$  exerted its protection by suppressing p- $\beta$ -catenin Ser37 function in the nucleus directly, but not by increasing the total  $\beta$ -catenin indirectly.

It is well known that ischemic cell death is a continuum of cell death at different stages with the morphological and biochemical features of both necrosis and apoptosis.<sup>2,38</sup> The early activation of caspases within 3 h of pMCAo<sup>39</sup> might push already injured cells into an inevitable death path via either canonical apoptosis or programmed necrosis as a result of molecular switch depending on energy supply.<sup>2,38</sup> The early upregulated 14-3-3 $\gamma$  might reduce acute ischemic cell death by suppressing either canonical apoptosis via the Bax-caspase 3 apoptotic pathway or necrosis via caspase 3-calpain interplay.<sup>40</sup> The delayed 14-3-3 $\gamma$  elevation at 24 h of pMCAo (Supplementary Figure 6a) might protect ischemic neurons from delayed ischemic cell death as indicated by the elevation of 14-3-3 $\gamma$  in survived ischemic neurons at 24 h of pMCAo (indicated by conclave arrowheads, Supplementary Figure 8).

In summary, we demonstrated that 14-3-3 $\gamma$  was an important inducible protective factor in OGD/ischemic neurons and promoted neuronal survival via a distinct nuclear mechanism, that is, the 14-3-3 $\gamma$ /p- $\beta$ -catenin Ser37/Bax pathway (Supplementary Figure 9). In OGD-treated astrocytes, 14-3-3 $\gamma$  protects astrocytes by binding to p-Bad Ser112,<sup>21</sup>

but neither via p- $\beta$ -catenin Ser 37 interaction (Supplementary Figure 10a) nor via Bax downregulation (Supplementary Figure 10b). Thus, targeting a common protective factor (i.e., 14-3-3 $\gamma$ ) but not a specific damaging factor (e.g., Bax or Bad) is likely to provide a desirable therapeutic effect for ischemic stroke.

#### Materials and Methods

**Plasmids and antibodies.** pcDNA-14-3-3 ( $\beta$ ,  $\epsilon$ ,  $\eta$ ,  $\gamma$ ,  $\sigma$ ,  $\tau$  and  $\zeta$ ) and pcDNA-difopein (dimeric 14-3-3 peptide inhibitor) plasmids were provided by Dr. Haian Fu (Emory University), and  $\beta$ -catenin was provided by Dr. Yasuyuki Fujita (University College London).  $\beta$ -catenin S37A was produced by point mutagenesis. 14-3-3 $\gamma$ -shRNA-1, 2 or 3 targeted to 5'-CGAGCAACTAGTGCAGAAA-3', 5'-CGGCGAAGGCAACAACCTAA-3' or 5'-CTGCTCCGAGACAACCTAA-3', respectively. 14-3-3 $\gamma$ -shRNA was constructed as previously reported.<sup>41</sup> N-con used corresponding scrambled sequences. All plasmids were confirmed by sequencing. Antibodies to 14-3-3 $\beta$ ,  $\epsilon$ ,  $\eta$ ,  $\gamma$ ,  $\tau$  and  $\zeta$  (Immuno-Biological Laboratories, Takasaki-Shi, Japan), p- $\beta$ -catenin Ser37, p-ASK-1 Ser966, p-p53 Ser315, cleaved caspase-3,  $\beta$ -catenin, p53 and NeuN (Cell Signaling Technology, Boston, MA, USA), Bax, p-Bad Ser112, green fluorescent protein and  $\beta$ -actin (Santa Cruz Biotechnology, Santa Cruz, CA, USA), p- $\beta$ -catenin Ser45 (Signalway Antibody, Baltimore, MD, USA) and Flag (Sigma, Saint Louis, MO, USA) were purchased.

#### Primary cultures of cerebral cortical neurons and nuclear-transfection.

Cultured rat cerebral cortical neurons were prepared from 16-day-old Sprague Dawley rat embryos as described.<sup>42</sup> Freshly isolated neurons ( $5 \times 10^6$ /35-mm dish) were transfected with plasmids by using the Nucleofector Kit and the Amaxa Nucleofector device (Lonza, Basel, Switzerland) according to the manufacturer's instructions.<sup>42</sup> Cultures were maintained in neurobasal media supplemented with 2% B27 and 2 mM L-glutamine (Invitrogen, Grand Island, NY, USA) 24 h after initial seeding, and half of the media was replenished every 2 days *in vitro* (DIV). The cultures were used for experiments at 7 DIV.

**OGD and cell death assay.** Primary neuronal cultures were washed with serum and glucose-free Dulbecco's modified Eagle's medium (DMEM) media (OGD media) (Invitrogen) three times and then incubated with OGD media in an

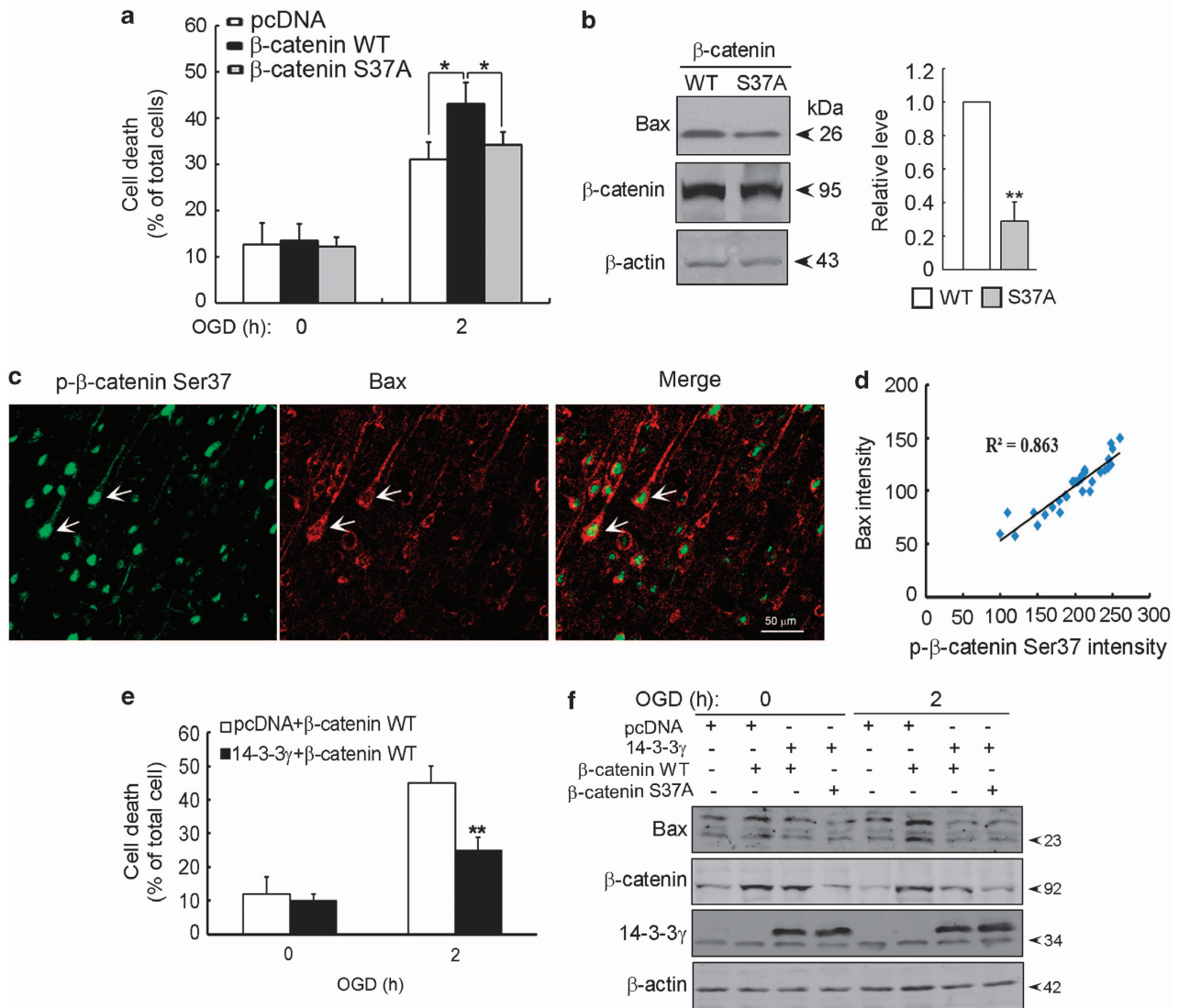


**Figure 8** 14-3-3 $\gamma$  suppresses p- $\beta$ -catenin Ser37-enhanced cell death and Bax expression in cortical neurons upon OGD. **(a)** Statistical analysis of cell death in cultured neurons upon OGD with  $\beta$ -catenin WT or S37A overexpression. Cell death was measured by PI staining. \* $P < 0.05$  versus pcDNA ( $n = 3$ ). **(b)** Representative western blot results and statistical analysis showing the effect of  $\beta$ -catenin WT or S37A overexpression on Bax expression in cultured neurons. Relative Bax level was normalized to that of  $\beta$ -actin. **(c)** Representative micrographs of double-fluorescent immunostaining showing the co-localization of p- $\beta$ -catenin Ser37 and Bax in cortical neurons in the Ipsi of 1 h-pMCAo rat. **(d)** Correlation of p- $\beta$ -catenin Ser37 and Bax levels in ischemic neurons in the Ipsi of 1 h-pMCAo rat. **(e)** Statistical analysis of the effect of 14-3-3 $\gamma$  overexpression on  $\beta$ -catenin-enhanced cell death in cultured cortical neurons upon 2 h of OGD. \* $P < 0.05$  versus pcDNA +  $\beta$ -catenin WT ( $n = 3$ ). **(f)** Representative western blot results showing the effect of 14-3-3 $\gamma$  overexpression on  $\beta$ -catenin-enhanced Bax expression in cultured cortical neurons upon 2 h of OGD

anaerobic chamber (Shanghai CIMO Medical Instrument Manufacturing, Shanghai, China) with 95% N<sub>2</sub>/5% CO<sub>2</sub> mixed gas.<sup>20,21</sup> Oxygen concentration in the anaerobic chamber was 0.1% as measured with a RSS-5100 (Shanghai Precision & Scientific Instrument, Shanghai, China) as reported previously.<sup>20</sup> Propidium iodide (PI, 1  $\mu$ g/ml) was used to distinguish dead cells in living cultures. Nuclei were stained with Hoechst 33342 (2  $\mu$ g/ml) to identify highly condensed apoptotic nuclei.<sup>21</sup>

**Western blot analysis.** Total soluble proteins were extracted from cultured cells or brain tissues by using radio-immunoprecipitation assay lysis buffer (Applygen Technologies Incorporation, Beijing, China) containing phenylmethanesulfonyl fluoride (Sigma). Equal amounts of total proteins were subjected to western blotting analysis as previously described.<sup>42</sup> The membranes were blocked with 5% (w/v) nonfat dried milk in Tris-buffered saline and then incubated with primary antibodies. After incubation with IRDye 800CW or IRDye 680CW conjugated goat anti-rabbit or anti-mouse IgG (Licor Biosciences, Lincoln, NE,

USA), the blots were visualized and quantified by using the Odyssey Infrared Imaging System (Licor Biosciences).

**Fluorescent immunostaining.** Brain sections or cultured neurons were fixed with 4% paraformaldehyde, permeabilized with 0.2% Triton X-100, blocked with 3% bovine serum albumin (BSA), incubated with primary antibodies overnight at 4 °C and then with the corresponding FITC- or rhodamine-conjugated secondary antibodies for 1 h at room temperature.<sup>42</sup> Micrographs were taken with a Zeiss 510 confocal microscope (Carl Zeiss, Oberkochen, Germany).

**Co-immunoprecipitation (Co-IP).** After OGD treatment, cultured neurons were washed once with cold PBS and lysed in 400  $\mu$ l of lysis buffer (20 mM Tris-HCl, pH 7.5, 50 mM NaCl, 50 mM NaF, 0.5 mM EDTA, 0.5% (v/v) Triton X-100 and protease inhibitors) per 35-mm dish. Supernatants were collected by centrifugation at 10 000  $\times$  g for 10 min at 4 °C. Four hundred micrograms of total soluble proteins in 400  $\mu$ l was incubated with 1  $\mu$ g of mouse anti-14-3-3 $\gamma$

antibodies overnight with gentle rotation at 4 °C.<sup>21</sup> Twenty microliters of 50% (v/v) protein G-agarose slurry was added and incubated for another 4 h with gentle rotation at 4 °C. The immunoprecipitates were collected by spin down and washed with ice-cold lysis buffer for five times. Twenty microliters of 2xSDS-PAGE gel loading buffer was used to dissociate proteins from the precipitates by boiling for 5 min. The supernatants were collected and subjected to western blot analysis with the corresponding antibodies.

**RT and quantitative PCR (qPCR).** Total RNA was extracted from cells or brain tissues using TRIZOL reagent (Invitrogen). Total RNA (2  $\mu$ g) was used to perform RT by using M-MLV transcriptase (Promega, Fitchburg, WI, USA) and oligo (dT15) primer (Promega) in a total volume of 20  $\mu$ l. Conventional PCR and qPCR were performed as described previously using  $\beta$ -actin as the internal control.<sup>43</sup> The primers used in PCR were Bax: 5'-CAGGATGCGTCCACCAAGA A-3' and 5'-GCAAAGTAGAAGAGGGCAACCAC-3'; Bad: 5'-GCAGCCACCAA CAGTCATCAT-3' and 5'-CAAACATCATCGCTCATCCTTCG-3'; Bcl-2: 5'-CGCT ACCGTCGTGACTTCGC-3' and 5'-CATCCCAGCCTCCGTTATCC-3'; Bcl-xL: 5'-T GCGTGGAAAGCGTAGACAAGG-3' and 5'-TGAAGAGTGAGCCAGCAGAAC-3'; myeloid cell leukemia sequence-1 (MCL-1): 5'-CTCTTATTTCTTCGGTGCCTT TG-3' and 5'-CCAGTCCCGTTTCGCTTACA-3',  $\beta$ -actin: 5'-CAGCCTTCTT CTGGGTAT-3' and 5'-GCTCAGTAACAGTCCGCCTA-3'. Triplicate measurements were collected for each sample and 14-3-3 mRNA was normalized to  $\beta$ -actin and then expressed as the fold of the corresponding control for each condition.

**Animals.** Animal studies were approved by the University Committee on Animal Resources of the University of Huazhong University of Science and Technology (HUST) and conducted in accordance with the NIH guidelines for the care and use of laboratory animals. Adult male SD rats (300 g–350 g) were purchased from the Animal Center of Tongji Medical College, HUST and housed in a 12:12 h light–dark cycled room maintained at 22  $\pm$  2 °C with food and water *ad libitum* for 5 days prior to the experiments.

**Permanent middle cerebral artery occlusion (pMCAo).** Focal brain ischemia was induced by MCAo as described previously.<sup>44</sup> Briefly, rats were anesthetized with 4% isoflurane and maintained with 2.5% isoflurane, 30% oxygen and 70% air via a face mask. After the right common carotid artery was exposed and its external branch was ligated, a monofilament nylon suture (0.24–0.26 mm in diameter) with poly-L-lysine was inserted into the internal carotid artery through the external carotid artery stump and advanced up to 18–20 mm or until resistance was felt. Sham-operated rats underwent the same surgical procedure without suture insertion. Rectal temperature was monitored throughout and maintained at 37.0  $\pm$  0.5 °C by a feedback-regulated heating system (Harvard Apparatus, Holliston, MA, USA). Physiological parameters (i.e., arterial pH, PaCO<sub>2</sub>, PaO<sub>2</sub>) were analyzed with 50  $\mu$ l of femoral artery blood by using an AVL OPTI 3 Blood Gas Analyzer (AVL Co., Plymouth, MI, USA) and monitored at three time points, that is, 5 min before MCAo, immediately after MCAo and 45 min after MCAo (Supplementary Figure 11a). Regional cerebral blood flow (CBF) was monitored at 2 mm posterior and 4 mm lateral to the bregma during MCAo by a Laser Doppler Perfusion Monitor (moorVMS-LDF2, Axminster, UK).<sup>45</sup> After the skull bone was thinned to translucency, the laser-doppler flowmeter probe was placed onto the brain surface of MCA blood supply region. CBF baseline was initially measured and stabilized for 10 min before the ligation of external carotid artery. Then, CBF was monitored throughout the filament insertion and a sharp decrease of CBF to <20% of the baseline was considered as successful MCAo<sup>45</sup> (Supplementary Figure 11b). The infarct was evaluated from 2-mm-thick coronal sections stained with 2% 2,3,5-TTC (Sigma).

**Immunohistochemistry (IHC).** Rat brains were perfused and post-fixed for 24 h in 4% paraformaldehyde. Brain slices cut into 20  $\mu$ m with a vibratome (S100, TPI; Leica, Wetzlar, Germany) were collected consecutively in PBS. Brain slices were treated with 0.3% H<sub>2</sub>O<sub>2</sub>/0.5% Triton X-100 in PBS for 10 min, blocked with 5% BSA/PBS for 30 min at room temperature, then incubated with primary antibodies overnight at 4 °C, followed by a biotin-labeled secondary antibody for 1 h. The immunoreaction was detected with a streptavidin-biotin-peroxidase complex and visualized with diaminobenzidine tetrachloride. Negative controls were subjected to the same procedures, but without primary antibody. For statistical analysis, all micrographs were taken with the same parameters (8 micrographs/section).<sup>43</sup> The integral optical density (IOD) of 14-3-3 staining

( $\times$  200 magnifications) was estimated using Image-Pro Plus 6.0 software (Media Cybernetics Inc., Rockville, MD, USA).<sup>43</sup> Mean IOD was calculated as IOD SUM/area. Relative 14-3-3 level in the Ipsi was compared to its Contra.

**Fluorescence resonance energy transfer (FRET).** FRET was conducted by using the acceptor photobleaching method with Zeiss FRET-Plus Version 4.0.4 software incorporated into a Zeiss 510 confocal microscope. Cultured cortical neurons were double-stained with mouse anti-14-3-3 $\gamma$  and rabbit anti-p- $\beta$ -catenin Ser37 or rabbit anti-Bax antibodies and the corresponding FITC- or TRITC-conjugated secondary antibodies. Selected regions of interest of neurons were bleached using the 543 nm laser at maximum intensity for 20 iterations and the donor/acceptor fluorescent images were collected before and after bleaching. The FRET efficiency was calculated, and an increase of 20% of the donor fluorescence after bleaching was considered as a positive FRET signal.<sup>46</sup>

**Neuronal N2a cell lines and lipofection.** Mouse neuroblastoma N2a cells were cultured in DMEM/Opti-M (V/V = 1:1) supplemented with 5% fetal bovine serum (Invitrogen). After 24 h, transfection was performed using Lipofectamine 2000 (Invitrogen) according to the manufacturer's instructions.<sup>41</sup>

**Statistical analysis.** For animal experiments, 5–8 animals/group were randomly selected. All experiments were repeated at least three times. All values were expressed as mean  $\pm$  S.E.M. Statistical analysis was performed with a two-way ANOVA followed by the Student–Newman–Keuls test, with  $P < 0.05$  considered significant.

## Conflict of Interest

The authors declare no conflict of interest.

**Acknowledgements.** This work was supported by grants from the National Natural Science Foundation of China (30470539, 30570555, 81070937, 81172397) and the Fundamental Research Funds for the Central Universities, HUST (No. 2013ZHYX017) to XQC; the National Natural Science Foundation of China (31070974 and 31171009), the Beijing Natural Science Foundation (7091004) and the National Basic Research Program of China (973 Program, 2011CB504400) to ACHY; the National Natural Science Foundation of China (81271509) and Shanghai Pujiang Program (11PJ1401800) from Science and Technology Commission of Shanghai Municipality to LQ.

- Adams Jr HP, del Zoppo G, Alberts MJ, Bhatt DL, Brass L, Furlan A et al. Guidelines for the early management of adults with ischemic stroke: a guideline from the American Heart Association/American Stroke Association Stroke Council, Clinical Cardiology Council, Cardiovascular Radiology and Intervention Council, and the Atherosclerotic Peripheral Vascular Disease and Quality of Care Outcomes in Research Interdisciplinary Working Groups: The American Academy of Neurology affirms the value of this guideline as an educational tool for neurologists. *Circulation* 2007; **115**: e478–e534.
- Lipton P. Ischemic cell death in brain neurons. *Physiol Rev* 1999; **79**: 1431–1568.
- Bederson JB, Pitts LH, Germano SM, Nishimura MC, Davis RL, Bartkowski HM. Evaluation of 2,3,5-triphenyltetrazolium chloride as a stain for detection and quantification of experimental cerebral infarction in rats. *Stroke* 1986; **17**: 1304–1308.
- Sandercock P, Wardlaw JM, Lindley RL, Dennis M, Cohen G, Murray G et al. The benefits and harms of intravenous thrombolysis with recombinant tissue plasminogen activator within 6 h of acute ischaemic stroke (the third international stroke trial [IST-3]): a randomised controlled trial. *Lancet* 2012; **379**: 2352–2363.
- Wardlaw JM, Murray V, Berge E, del Zoppo G, Sandercock P, Lindley RL et al. Recombinant tissue plasminogen activator for acute ischaemic stroke: an updated systematic review and meta-analysis. *Lancet* 2012; **379**: 2364–2372.
- Tissue plasminogen activator for acute ischaemic stroke. The National Institute of Neurological Disorders and Stroke rt-PA Stroke Study Group. *N Engl J Med* 1995; **333**: 1581–1587.
- Fisher M. New approaches to neuroprotective drug development. *Stroke* 2011; **42**(Suppl): S24–S27.
- Stankowski JN, Gupta R. Therapeutic targets for neuroprotection in acute ischemic stroke: lost in translation? *Antioxid Redox Signal* 2011; **14**: 1841–1851.
- Faden AI, Stoica B. Neuroprotection: challenges and opportunities. *Arch Neurol* 2007; **64**: 794–800.
- Dong Y, Zhao R, Chen XQ, Yu AC. 14-3-3 $\gamma$  and neuroglobin are new intrinsic protective factors for cerebral ischemia. *Mol Neurobiol* 2010; **41**: 218–231.

11. Masters SC, Fu H. 14-3-3 proteins mediate an essential anti-apoptotic signal. *J Biol Chem* 2001; **276**: 45193–45200.
12. Gelperin D, Weigle J, Nelson K, Roseboom P, Irie K, Matsumoto K *et al*. 14-3-3 proteins: potential roles in vesicular transport and Ras signaling in *Saccharomyces cerevisiae*. *Proc Natl Acad Sci USA* 1995; **92**: 11539–11543.
13. Li Z, Zhao J, Du Y, Park HR, Sun SY, Bernal-Mizrachi L *et al*. Down-regulation of 14-3-3zeta suppresses anchorage-independent growth of lung cancer cells through anoikis activation. *Proc Natl Acad Sci USA* 2008; **105**: 162–167.
14. Morrison DK. The 14-3-3 proteins: integrators of diverse signaling cues that impact cell fate and cancer development. *Trends Cell Biol* 2009; **19**: 16–23.
15. Fu H, Subramanian RR, Masters SC. 14-3-3 proteins: structure, function, and regulation. *Annu Rev Pharmacol Toxicol* 2000; **40**: 617–647.
16. Tzivion G, Shen YH, Zhu J. 14-3-3 proteins; bringing new definitions to scaffolding. *Oncogene* 2001; **20**: 6331–6338.
17. Wilftang J, Otto M, Baxter HC, Bodemer M, Steinacker P, Bahn E *et al*. Isoform pattern of 14-3-3 proteins in the cerebrospinal fluid of patients with Creutzfeldt-Jakob disease. *J Neurochem* 1999; **73**: 2485–2490.
18. Jayaratnam S, Khoo AK, Basic D. Rapidly progressive Alzheimer's disease and elevated 14-3-3 proteins in cerebrospinal fluid. *Age Ageing* 2008; **37**: 467–469.
19. Yacoubian TA, Slone SR, Harrington AJ, Hamamichi S, Schieltz JM, Caldwell KA *et al*. Differential neuroprotective effects of 14-3-3 proteins in models of Parkinson's disease. *Cell Death Dis* 2010; **1**: e2.
20. Chen XQ, Fung YW, Yu AC. Association of 14-3-3 $\gamma$  and phosphorylated bad attenuates injury in ischemic astrocytes. *J Cereb Blood Flow Metab* 2005; **25**: 338–347.
21. Chen XQ, Chen JG, Zhang Y, Hsiao WW, Yu AC. 14-3-3 $\gamma$  is upregulated in *in vitro* ischemia and binds to protein kinase Raf in primary cultures of astrocytes. *Glia* 2003; **42**: 315–324.
22. Umahara T, Uchihara T, Tsuchiya K, Nakamura A, Iwamoto T. Intracellular localization and isoform-dependent translocation of 14-3-3 proteins in human brain with infarction. *J Neurol Sci* 2007; **260**: 159–166.
23. Bose P, Thakur S, Thalappilly S, Ahn BY, Satpathy S, Feng X *et al*. ING1 induces apoptosis through direct effects at the mitochondria. *Cell Death Dis* 2013; **4**: e837.
24. Zhao H, Shimohata T, Wang JQ, Sun G, Schaal DW, Sapolsky RM *et al*. Akt contributes to neuroprotection by hypothermia against cerebral ischemia in rats. *J Neurosci* 2005; **25**: 9794–9806.
25. Xi L, Taher M, Yin C, Salloum F, Kukreja RC. Cobalt chloride induces delayed cardiac preconditioning in mice through selective activation of HIF-1 $\alpha$  and AP-1 and iNOS signaling. *Am J Physiol Heart Circ Physiol* 2004; **287**: H2369–H2375.
26. Valsecchi V, Pignataro G, Del Prete A, Sirabella R, Matrone C, Boscia F *et al*. NCX1 is a novel target gene for hypoxia-inducible factor-1 in ischemic brain preconditioning. *Stroke* 2011; **42**: 754–763.
27. Mhaweche P. 14-3-3 proteins—an update. *Cell Res* 2005; **15**: 228–236.
28. Nomura M, Shimizu S, Sugiyama T, Narita M, Ito T, Matsuda H *et al*. 14-3-3 interacts directly with and negatively regulates pro-apoptotic Bax. *J Biol Chem* 2003; **278**: 2058–2065.
29. Zha J, Harada H, Yang E, Jockel J, Korsmeyer SJ. Serine phosphorylation of death agonist BAD in response to survival factor results in binding to 14-3-3 not BCL-X(L). *Cell* 1996; **87**: 619–628.
30. Krieghoff E, Behrens J, Mayr B. Nucleo-cytoplasmic distribution of beta-catenin is regulated by retention. *J Cell Sci* 2006; **119**(Pt 7): 1453–1463.
31. Wodarz A, Nusse R. Mechanisms of Wnt signaling in development. *Annu Rev Cell Dev Biol* 1998; **14**: 59–88.
32. Klaus A, Birchmeier W. Wnt signalling and its impact on development and cancer. *Nat Rev Cancer* 2008; **8**: 387–398.
33. Saikumar P, Dong Z, Weinberg JM, Venkatachalam MA. Mechanisms of cell death in hypoxia/reoxygenation injury. *Oncogene* 1998; **17**: 3341–3349.
34. Lin CH, Lu YZ, Cheng FC, Chu LF, Hsueh CM. Bax-regulated mitochondria-mediated apoptosis is responsible for the *in vitro* ischemia induced neuronal cell death of Sprague Dawley rat. *Neurosci Lett* 2005; **387**: 22–27.
35. Wang Z, Gall JM, Bonegio R, Havasi A, Illanes K, Schwartz JH *et al*. Nucleophosmin, a critical Bax cofactor in ischemia-induced cell death. *Mol Cell Biol* 2013; **33**: 1916–1924.
36. Tian Q, Feetham MC, Tao WA, He XC, Li L, Aebersold R *et al*. Proteomic analysis identifies that 14-3-3zeta interacts with beta-catenin and facilitates its activation by Akt. *Proc Natl Acad Sci USA* 2004; **101**: 15370–15375.
37. Cappuccio I, Calderone A, Busceti CL, Biagioni F, Pontarelli F, Bruno V *et al*. Induction of Dickkopf-1, a negative modulator of the Wnt pathway, is required for the development of ischemic neuronal death. *J Neurosci* 2005; **25**: 2647–2657.
38. Puyal J, Ginet V, Clarke PG. Multiple interacting cell death mechanisms in the mediation of excitotoxicity and ischemic brain damage: a challenge for neuroprotection. *Prog Neurobiol* 2013; **105**: 24–48.
39. Benchoua A, Guégan C, Couriaud C, Hosseini H, Sampaio N, Morin D *et al*. Specific caspase pathways are activated in the two stages of cerebral infarction. *J Neurosci* 2001; **21**: 7127–7134.
40. Sun M, Zhao Y, Xu C. Cross-talk between calpain and caspase-3 in penumbra and core during focal cerebral ischemia-reperfusion. *Cell Mol Neurobiol* 2008; **28**: 71–85.
41. Ye SQ, Zhou XY, Lai XJ, Zheng L, Chen XQ. Silencing neuroglobin enhances neuronal vulnerability to oxidative injury by down-regulating 14-3-3 $\gamma$ . *Acta Pharmacol Sin* 2009; **30**: 913–918.
42. Li L, Liu QR, Xiong XX, Liu JM, Lai XJ, Cheng C *et al*. Neuroglobin promotes neurite outgrowth via differential binding to PTEN and Akt. *Mol Neurobiol* 2014; **49**: 149–162.
43. Zhang J, Lan SJ, Liu QR, Liu JM, Chen XQ. Neuroglobin a novel intracellular hexa-coordinated globin, functions as a tumor suppressor in hepatocellular carcinoma via Raf/MAPK/Erk. *Mol Pharmacol* 2013; **83**: 1109–1119.
44. Li Y, Chopp M, Jiang N, Yao F, Zaloga CJ. Temporal profile of *in situ* DNA fragmentation after transient middle cerebral artery occlusion in the rat. *J Cereb Blood Flow Metab* 1995; **15**: 389–397.
45. Cheng J, Uchida M, Zhang W, Grate MR, Herson PS, Hurn PD. Role of salt-induced kinase 1 in androgen neuroprotection against cerebral ischemia. *J Cereb Blood Flow Metab* 2011; **31**: 339–350.
46. Hu S, Yang H, Cai R, Liu Z, Yang X. Biotin induced fluorescence enhancement in resonance energy transfer and application for bioassay. *Talanta* 2009; **80**: 454–458.



**Cell Death and Disease** is an open-access journal published by Nature Publishing Group. This work is licensed under a Creative Commons Attribution-NonCommercial-ShareAlike 3.0 Unported License. The images or other third party material in this article are included in the article's Creative Commons license, unless indicated otherwise in the credit line; if the material is not included under the Creative Commons license, users will need to obtain permission from the license holder to reproduce the material. To view a copy of this license, visit <http://creativecommons.org/licenses/by-nc-sa/3.0/>

Supplementary Information accompanies this paper on Cell Death and Disease website (<http://www.nature.com/cddis>)